Cationic and charge segregation in $La_{2/3}Ca_{1/3}MnO_3$ thin films grown on (001) and (110) $SrTiO_3$

S. Estradé,[1,a] J. Arbiol,[1] F. Peiró,[1] I. C. Infante,[2] F. Sánchez,[2] J. Fontcuberta,[2] F. de la Peña,[3] M. Walls,[3] and C. Colliex[3]
[1]*EME/CeRMAE/IN²UB, Departament d'Electrònica, Universitat de Barcelona, Martí i Franquès 1, 08028 Barcelona, CAT, Spain*
[2]*Institut de Ciència de Materials de Barcelona-CSIC, 08193 Bellaterra, CAT, Spain*
[3]*Laboratoire de Physique des Solides, UMR CNRS 8502, Bâtiment 510, Université Paris Sud, 91405 Orsay, France*

(Received 10 April 2008; accepted 24 August 2008; published online 18 September 2008)

Electron energy-loss spectroscopy is used to map composition and electronic states in epitaxial $La_{2/3}Ca_{1/3}MnO_3$ films grown on $SrTiO_3$ (001) and (110) substrates. It is found that in partially relaxed (110) films cationic composition and valence state of $Mn^{3+/4+}$ ions are preserved across the film thickness. In contrast, in fully strained (001) films, the Ca/La ratio gradually changes across the film, being La rich at film/substrate interface and La depleted at free surface; Mn valence state changes accordingly. These observations suggest that a strongly orientation-dependent adaptative composition mechanism dominates stress accommodation in manganite films and provides microscopic understanding of their dissimilar magnetic properties. © *2008 American Institute of Physics*. [DOI: 10.1063/1.2981574]

Mixed-valence ferromagnetic manganite films, such as $La_{2/3}Ca_{1/3}MnO_3$ (LCMO), have been the object of much attention in recent years due to their potential applications in spintronics.[1,2] However, expectations have been lowered by the negligible room-temperature magnetoresistance in tunnel junctions.[3] Although the reasons for this behavior are not yet fully known, it has been suggested that they may be linked to electronic phase separation.[4] Electron energy-loss spectroscopy (EELS) allows direct determination of local Mn oxidation state and composition at the subnanometric scale. Several EELS studies on epitaxial (001) manganite thin films have been reported in literature. Early experiments by Pailloux *et al.*[5] observed no variation in Mn oxidation state at the STO($SrTiO_3$)/LSMO($La_{2/3}Sr_{1/3}MnO_3$) interface. Simon *et al.*[6] observed migration of Ca^{2+} toward manganite-free surface in (001) textured LCMO/STO($SrTiO_3$)/LCMO structures, whereas Maurice *et al.*[7] and Samet *et al.*[8] found no cation migration in the LSMO ($La_{2/3}Sr_{1/3}MnO_3$)/STO/LSMO system but found a weak decrease in the Mn valence near the interfaces, attributed to a transfer of electrons from STO to LSMO. It has been observed that in LCMO films grown on $LaAlO_3$ substrates, which are under compressive strain, the La^{3+} ions migrate toward the top layer surface.[9] Little attention was received, so far, by the chemistry and electronic structure of (110) LCMO films, reported to display enhanced magnetic properties when compared to their (001) counterparts.[10,11] In this work, we report detailed transmission electron microscopy (TEM) and EELS analyses of epitaxial LCMO layers grown simultaneously on (001) and (110) STO substrates.

The (001) and (110) LCMO layers were grown by rf sputtering at 800 °C, at 330 mtorr, with an O_2/Ar pressure ratio of $\frac{1}{4}$ and a growth rate of ~0.4 nm/min. After growth, *in situ* annealing was performed at 800 °C for 1 h in O_2 atmosphere at 350 torr.[10] The magnetic properties of these films have been previously studied.[10,11] both magnetization [Fig. 1(a)] and Curie temperature of the (110) films are much larger than those of their (001) counterparts. LCMO films, when grown on (001) and (110) STO substrates, have identical (tensile) lattice mismatch (~1.1%). However, whereas in-plane orthogonal directions [100] and [010] of (001) films are equivalent, [001] and [1$\bar{1}$0] directions are not equivalent

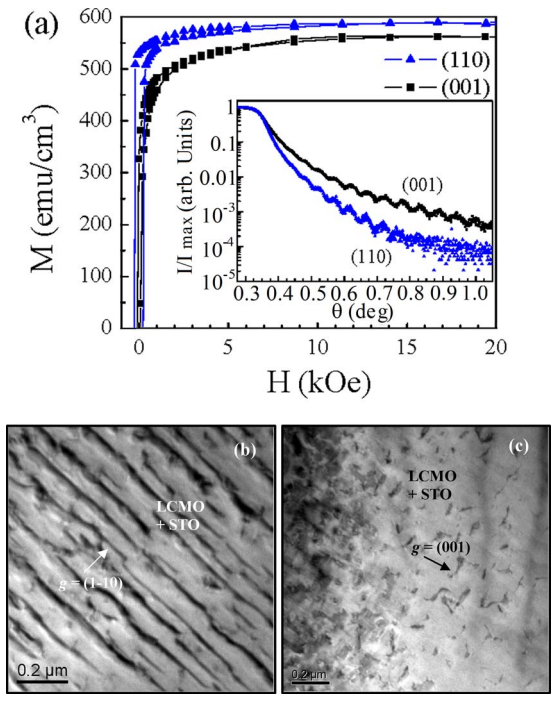

FIG. 1. (Color online) (a) Magnetization vs field curves in the −1–20 kOe range for (001) LCMO (squares) and (110) LCMO (triangles) 80 nm films measured at 10 K. Magnetic field was applied in-plane of the samples, being parallel to [100] direction for the (001) films and to [001] direction for the (110) film. Inset: Normalized XRR spectra from (001) (squares) and (110) (triangles) 85 nm films. (b) $g=(1-10)$ and (c) $g=(011)$ two beam images of [110] LCMO/STO in PV geometry.

[a]Electronic mail: sestrade@el.ub.es.

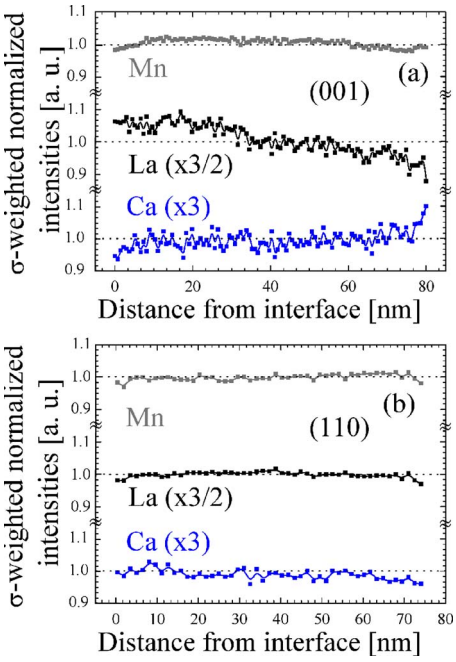

FIG. 2. (Color online) Mn, La, and Ca σ-weighted intensities along the layers, for (a) (001) and (b) (110) orientations. To get identical range of relative variations in all cation concentrations visible in the plot, data for La and Ca have been multiplied by $(x3/2)$ and $(x3)$, respectively.

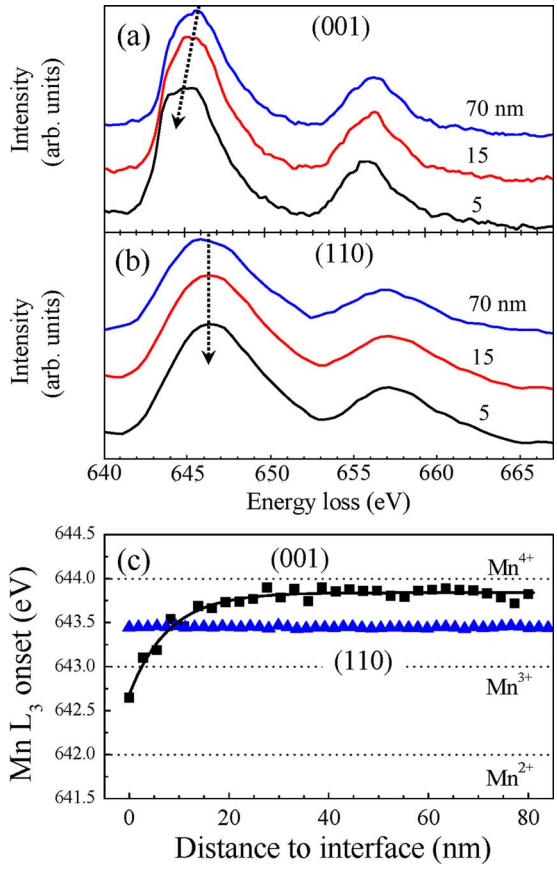

FIG. 3. (Color online) Mn $L_{3,2}$ EELS spectra at the indicated positions across the film (at 5, 15, and 70 nm from the substrate/film interface) for the (a) (001) LCMO and (b) (110) LCMO films. Arrows in (a) and (b) are eye guides. (c) Position dependent Mn L_3 edge onset across film thickness for (001) and (110) films. Edge onset was determined at full width at half maximum of L_3 edge.

for (110) films, and have different Young's moduli.

TEM samples, prepared in cross section geometry by focused ion beam (FIB) and in plan-view (PV) geometry by mechanical thinning down to 25 μm and Ar+ bombardment at $V=5$ kV and 7° using a PIPS-Gatan, were observed in a Jeol J2010F scanning TEM (STEM) microscope, with a hot field emission gun at 200 keV. EELS spectra and STEM images were obtained in a VG 501 dedicated STEM. Ca, La, and Mn normalized σ-weighted intensities (nW intensities) were obtained from EELS spectra as I_X/σ_X, normalized to the value of the mean Mn σ-weighted intensity along the layers. I_X, the integrated intensities of background substracted Ca $L_{3,2}$, La $M_{5,4}$, and Mn $L_{3,2}$ edges, and σ_X is the cross section for each edge (calculated using Gatan Digital Micrograph software). The Mn L_3 EELS edge position and Mn L_3/Mn L_2 edge intensity ratio were determined using MANGANITAS (Refs. 9 and 12) software package.

X-ray reflectometry (XRR) measurements [Fig. 1(a), inset] were used to determine film thickness. From the observed reflectivity oscillations, layer thickness was determined to be about 80 and 82 nm for (001) and (110) films, respectively. A faster decrease in the reflected intensity in the (110) film indicates[13] a relatively higher roughness. Exhaustive x-ray diffraction (XRD) and electron diffraction experiments showed[10] that the LCMO films grow on (001) and (110) STO substrates in a "cube-on-cube" mode with the following epitaxial relationships: LCMO(001) $\times$[100]$\|$STO(001)[100] and LCMO(110)[001]$\|$STO(110) $\times$[001], respectively.

PV TEM study of (001) sample showed no evidence of defects. This is in good agreement with XRD lattice parameter measurements,[10] which indicated that (001) film is fully and isotropically in-plane strained. Yet, for (110) film, $g=(1-10)$ two beam observation [Fig. 1(b)] shows a highly periodic distribution of misfit dislocations running perpendicular to the $[1\bar{1}0]$ direction (which seems to be in good agreement with recent reports);[14] $g=(001)$ two beam observation [Fig. 1(c)] shows a much lower density of dislocations, running perpendicular to (001). XRD measurements of the (110) LCMO films indicated an anisotropic partial in-plane relaxation: strain $\sim+0.34\%$ in $[1\bar{1}0]$ direction and $\sim+0.62\%$ in [001] direction.[10]

Composition profiles across film thickness were obtained by EELS from cross sections. First, spectra (in the range of 325 to 870 eV) were acquired along the direction perpendicular to the substrate/film interface. Concentrations of the different species at different positions were determined from these spectra. The Mn, Ca, and La σ-weighted intensities along the layers are depicted, for (001) and (110) films, in Fig. 2. In (110) film [Fig. 2(b)], Mn, Ca, and La concentrations are found to be clearly constant, and Ca and La nW intensities are close to the expected values ($\sim$0.33 and $\sim$0.66) across the whole film. In contrast [Fig. 2(a)], for (001) films, a monotonous diminishing of the La nW intensity across film thickness is found, with interface (La enriched) and free surface (La deficient). It is also observed that the Ca nW intensity increases with distance to interface.

EELS spectra in the (500–675) eV energy-loss range, where Mn $L_{2,3}$ edges (640 and 651 eV) and O K edge (532 eV) occur, were also recorded. The positions of the Mn $L_{2,3}$ edges are known to be related to the Mn oxidation state.[9,15–20] In Fig. 3 we show representative EELS spectra of

the (001) and (110) LCMO films [Figs. 3(a) and 3(b), respectively]. The Mn $L_{2,3}$ doublet remains at constant energy across the (110) film. In sharp contrast, for (001) films [Fig. 3(a)], it progressively shifts toward lower energies when approaching LCMO/STO interface [Fig. 3(b)]. Mn L_3 edge positions are collected in Fig. 3(c). No significant variation is found for (110) films. Dotted lines in Fig. 3(c) indicate the Mn $L_{2,3}$ edge energies reported in literature[18–20] for Mn^{m+} ions in various oxidation states. The oxidation state of Mn^{m+} ions is constant across (110) films but gradually changes in (001) films, with a progressive reduction in the Mn^{m+} species near the interface while free surface appears to be overoxidized. The variation in the Mn L_3/Mn L_2 intensity ratio (the ratio decreases with oxidation state)[18,19] provides further confirmation of the reduction in Mn^{m+} close to the interface in (001) films, as it decreases from 3.7 ± 0.1 near interface to 2.3 ± 0.1 near free surface. The observed variation in Mn^{m+} oxidation state in (001) layer is fully consistent with the detected La enrichment near the interface. Present data cannot exclude additional Mn^{m+} reduction at the interface as a result of a possible transfer of electrons from STO substrate.[7,8]

In Fig. 1(a) (main panel), we show the magnetization versus field at 10 K for (001) and (110) 80 nm films. The saturation magnetization value of the (110) LCMO film ($\approx$588 emu/cm^3) is higher than that of the (001) LCMO film ($\approx$560 emu/cm^3). The presence of La-rich and La-poor regions in (001) films leads to electronic phase segregation and occurrence of nonferromagnetic phases, as evidenced by nuclear magnetic resonance experiments.[4,11]

As the stressed (001) sample does not exhibit plastic relaxation, it seems that elastic strain accommodation has occurred via cation migration. These results are in good agreement with the findings of Simon *et al.*,[6] and represent a solid experimental confirmation of the trends observed there. Yet, in the present work, the strain acting on the films has been changed without changing the composition of the film. We notice that due to the larger ionic size of La^{3+} than Ca^{2+}, La^{3+} enrichment close to the STO interface (Fig. 2) provides a natural mechanism for cell-parameter matching to STO substrate. Comparison between the two encountered stress accommodation mechanisms, namely, defect formation for (110) orientation and cation migration for (001) orientation, in two systems with the same layer/substrate mismatch and grown in the same conditions, strongly suggests that strain accommodation via cation migration is more detrimental to the magnetic performance than accommodation via defect creation, both because it is less effective (i.e., layers remain in higher strain conditions) and because it modifies the optimal hole doping $\left(\sim\frac{1}{3}\right)$ in extensive regions of (001) films.

Support from European Union project ESTEEM allowed us to perform STEM measurements in the LPS (France). Financial support by the MEC of the Spanish Government Projects (Grant Nos. NAN2004-9094-C03, MAT2005-5656-C04, and NANOSELECT CSD2007-00041) and by the European Union [project MaCoMuFi (Grant No. FP6-03321) and FEDER] are acknowledged. The BRD grant program of Universitat de Barcelona is also acknowledged. We are very thankful to Dr. A. Romano-Rodríguez for FIB sample preparation.

[1] J. S. Moodera and G. Mathon, J. Magn. Magn. Mater. **200**, 248 (1999).
[2] S. S. P. Parkin, K. P. Roche, M. G. Samant, P. M. Rice, R. B. Byers, R. E. Scheuerlein, E. J. O'Sullivan, S. L. Brown, J. Bucchigano, D. W. Abraham, Y. Lu, M. Rooks, P. L. Trouilloud, R. A. Wanner, and W. J. Gallagher, J. Appl. Phys. **85**, 5828 (1999).
[3] M. Viret, M. Drouet, J. Nassar, J. P. Contour, C. Fermon, and A. Fert, Europhys. Lett. **39**, 545 (1997).
[4] M. Bibes, L. Balcells, S. Valencia, J. Fontcuberta, M. Wojcik, E. Jedryka, and S. Nadolski, Phys. Rev. Lett. **87**, 067210 (2001).
[5] F. Pailloux, D. Imhoff, T. Sikora, A. Barthélémy, J.-L. Maurice, J.-P. Contour, C. Colliex, and A. Fert, Phys. Rev. B **66**, 014417 (2002).
[6] J. Simon, T. Walther, W. Mader, J. Klein, D. Reisinger, L. Alff, and R. Gross, Appl. Phys. Lett. **84**, 3882 (2004).
[7] J.-L. Maurice, D. Imhoff, J.-P. Contour, and C. Colliex, Philos. Mag. **86**, 2127 (2006).
[8] L. Samet, D. Imhoff, J.-L. Maurice, J.-P. Contour, A. Gloter, T. Manoubi, A. Fert, and C. Colliex, Eur. Phys. J. B **34**, 179 (2003).
[9] S. Estradé, J. Arbiol, F. Peiró, Ll. Abad, V. Laukhin, L. Balcells, and B. Martínez, Appl. Phys. Lett. **91**, 252503 (2007).
[10] J. Fontcuberta, I. C. Infante, V. Laukhin, F. Sánchez, M. Wojcik, and E. Jedryka, J. Appl. Phys. **99**, 08A701 (2006).
[11] I. C. Infante, F. Sánchez, J. Fontcuberta, M. Wojcik, E. Jedryka, S. Estradé, F. Peiró, J. Arbiol, V. Laukhin, and J. P. Espinós, Phys. Rev. B **76**, 224415 (2007).
[12] R. F. Egerton, *Electron Energy-Loss Spectroscopy in the Electron Microscope*, 2nd ed. (Kluwer, Dordrecht, 1996).
[13] U. Pietsch, V. Holý, and T. Baubach, *High Resolution X-ray Scattering, from Thin Films to Lateral Nanostructures* (Springer, New York, 2004), pp. 98 and 143.
[14] Y. Y. Tse, R. I. Chakalov, M. M. Joshi, I. P. Jones, C. M. Muirhead, and R. Palai, J. Phys.: Conf. Ser. **26**, 115 (2006).
[15] Y. Q. Wang, X. F. Duan, Z. H. Wang, and B. G. Shen, Mater. Sci. Eng., A **333**, 80 (2002).
[16] Z. L. Wang, J. Bentley, and N. D. Evans, Micron **31**, 355 (2000).
[17] Z. L. Wang, J. S. Yin, and Y. D. Jiang, Micron **31**, 571 (2000).
[18] H. Kurata and C. Colliex, Phys. Rev. B **48**, 2102 (1993).
[19] V. Marchetti, J. Ghanbaja, P. Gérardin, and B. Loubinoux, Holzforschung **54**, 553 (2000).
[20] J. L. Maurice, F. Pailloux, A. Barthélémy, O. Durand, D. Imhoff, R. Lyonnet, A. Rocher, and J. P. Contour, Philos. Mag. **83**, 3201 (2003).